Gene Expression Profiling of Purified Rat Retinal Ganglion Cells

Ronald H. Farkas,[1,2] *Jiang Qian,*[1,2] *Jeffrey L. Goldberg,*[3,4] *Harry A. Quigley,*[1,5] *and Donald J. Zack*[1,2,6,7,8]

Purpose. The phenotype of specialized cells arises, in part, from their characteristic gene expression patterns. Retinal ganglion cells (RGCs) are of wide interest in neuroscience and die in glaucoma and other optic neuropathies. In this study the genes expressed by RGCs were profiled by expressed sequence tag (EST) analysis.

Methods. ESTs were generated from a cDNA library constructed from RGCs isolated by immunopanning. The RGC genes were compared with published microarray expression profiles from 13 different neural regions. Immunohistochemistry was performed by standard methods.

Results. Clustering of 4791 RGC ESTs identified 2360 unique gene clusters. Of these, 60% represented known genes, 27% uncharacterized genes/ESTs, and 13% novel sequence. Unexpectedly, one of the largest RGC clusters, RESP18, corresponded to a neuroendocrine-specific gene preferentially expressed in the hypothalamus. RESP18 immunoreactivity within the retina was found mainly in the RGC layer. DDAH1, a gene involved in nitric oxide metabolism, was localized to RGC and amacrine layers. Comparison of gene expression patterns across neuronal regions revealed a prominent subset of RGC genes that were overexpressed in dorsal root and trigeminal ganglia. To narrow the search for candidate disease-related genes, RGC genes were mapped to known disease loci for optic neuropathies.

Conclusions. This work is one of the first efforts to profile gene expression in a purified population of retinal neurons, the RGCs. The profiling, in addition to revealing both known and novel genes underlying the RGC phenotype, also uncovered common patterns of gene expression between RGCs and other sensory ganglia. (*Invest Ophthalmol Vis Sci.* 2004;45: 2503–2513) DOI:10.1167/iovs.03-1391

Retinal ganglion cells (RGCs) perform the final steps of retinal vision processing before carrying the visual signal to higher centers in the brain. The death of RGCs is a common cause of visual disability, most often occurring from glaucoma, a leading cause of irreversible blindness in developed countries and worldwide.[1,2] RGC death also occurs in many other optic neuropathies, which can be of environmental and/or genetic origin, with inheritance patterns ranging from mitochondrial to autosomal dominant. RGCs are widely used as a model system for neurobiological studies of development, trauma, and neuronal degeneration and regeneration. Thus, knowledge of RGC functions is important to the understanding of many neuronal processes.

The behavior of RGCs, and of all cells on a fundamental level, arises in large part from the specific distribution of genes that the cells express. Relatively little is known about the genes expressed by RGCs. Gene expression studies have been performed on the retina as a whole,[3] using a variety of methods, including expressed sequence tag (EST) sequencing,[4–6] serial analysis of gene expression (SAGE),[7,8] and microarrays.[9–13] However, the retina is a complex tissue composed of neuronal, glial, and vascular cell types. The dominant cell type of the retina is the photoreceptor, with RGCs comprising 5% or less of all retinal cells.[14,15] Thus, gene expression profiles from whole retina are unrepresentative of RGC gene expression. Previous efforts to identify the complete picture of retinal gene expression may have missed important RGC genes, due to the low relative frequency of RGCs and, hence, their mRNA transcripts.

Efforts to document gene expression of specific cell types in the eye have used EST sequencing from libraries derived separately from lens, iris, and retinal pigment epithelium-choroid.[4] Similarly, optic nerve astrocytes isolated from human retina have been studied with microarrays.[16] Efforts are currently underway to identify the expression pattern of single retinal cells.[17] Gene expression profiling has been undertaken for different subregions of the brain[18–25] and auditory system,[26] with the use of message amplification for cells microdissected individually[20,22,27,28] or purified by fluorescence-activated cell sorting.[29]

We describe herein an initial gene expression profile of rat RGCs that were separated from other cell types by immunopanning. RGCs purified by this method have provided information on the interactions that govern RGC physiology and development.[30] Through EST sequencing of a cDNA library prepared from purified RGCs, we found expression of both known and novel genes and have begun further investigation of how these genes relate to RGC function.

Materials and Methods

RGC cDNA Library

All experiments were conducted with adherence to the ARVO Statement for the Use of Animals in Ophthalmic and Vision Research. RGCs

From the [1]Department of Ophthalmology, Wilmer Eye Institute, the [2]Guerrieri Center for Genetic Engineering and Molecular Ophthalmology, and the [5]Dana Center for Preventive Ophthalmology at the Wilmer Eye Institute, Baltimore, Maryland; the Departments of [6]Molecular Biology and Genetics, [7]Neuroscience, and the [8]McKusick-Nathans Institute of Genetic Medicine, Johns Hopkins University School of Medicine, Baltimore, Maryland; and the [3]Department of Neurobiology, Stanford University, Stanford, California.

[4]Present affiliation: Bascom Palmer Eye Institute, McKnight Vision Research Center, Miami, Florida.

Supported by grants from the National Eye Institute, Glaucoma Foundation, Glaucoma Research Foundation, the American Health Assistance Foundation, and Santen Pharmaceutical, and by generous gifts from Mr. and Mrs. Marshall and Stevie Wishnack and from Mr. and Mrs. Robert and Clarice Smith. HAQ is the A. Edward Maumenee Professor of Ophthalmology; DJZ is the Guerrieri Professor of Genetic Engineering and Molecular Ophthalmology and is a recipient of a Research to Prevent Blindness Senior Investigator Award.

Submitted for publication December 23, 2003; revised March 2, 2004; accepted March 12, 2004.

Disclosure: **R.H. Farkas**, None; **J. Qian**, None; **J.L. Goldberg**, None; **H.A. Quigley**, None; **D.J. Zack**, None

The publication costs of this article were defrayed in part by page charge payment. This article must therefore be marked "*advertisement*" in accordance with 18 U.S.C. §1734 solely to indicate this fact.

Corresponding author: Ronald H. Farkas, Department of Ophthalmology, Wilmer Eye Institute, Maumenee 813, Johns Hopkins University School of Medicine, Baltimore, MD 21287; rfarkas@jhmi.edu.

from postnatal day (P)21 Sprague-Dawley rats (Simonsen Laboratories, Gilroy, CA) were purified by sequential immunopanning using a monoclonal antibody to Thy1.1, by a method that has been reported to yield approximately 99% purity.[30–33] Briefly, whole retina tissue was removed from rats from four litters, incubated in a papain solution, dissociated into single-cell suspension, and subjected to negative selection with anti-macrophage antiserum (1:100; Axell Accurate Chemical and Scientific Corp, Westbury, NY) to remove macrophage and endothelial cells. Remaining cells were then placed on panning plates containing Thy1.1 antibody, and unbound cells were removed with washing. RGCs were released after incubation with a trypsin solution. RGCs were cultured overnight on poly-D-lysine (Sigma-Aldrich) and laminin (Invitrogen-Gibco, Grand Island, NY), in serum-free defined medium, as described.[31,32] The yield of RGC cells was between 50% and 70%, with a survival of more than 90%.[31] Total RNA was extracted and confirmed to be intact by denaturing gel electrophoresis. The total RNA was reverse transcribed, and a nonnormalized, nonsubtracted cDNA library was constructed from 1 μg total RNA using SMART technology and 16 rounds of PCR amplification (BD Biosciences-Clontech, Palo Alto, CA). This method is based on template-switching at the 5′ end of the mRNA transcript, with binding of an anchor sequence that can serve as a priming site for PCR. The cDNA was then size fractionated and ligated into pDNR-LIB plasmid (BD Biosciences-Clontech). *Escherichia coli* (Electromax DH10B; Invitrogen, San Diego, CA) was transformed by electroporation and grown for 1 hour in SOC medium without further amplification. Clones were plated and randomly chosen for 5′ sequencing (Michigan State University Genomics Facility, East Lansing, MI, or Integrated Genomics GmbH, Jena, Germany). RGC EST sequences were submitted to the National Center for Biotechnology Information (NCBI; accession numbers CF974889 to CF9749532).

EST Sequence Clustering

Our clustering procedure consisted of two steps. First, the CAP3 sequence assembly program[34] was used with stringent criteria: overlap length of 200 bp and sequence identity percentage of 95% (command line options: -o 200 -p 95). Then, the sequence clusters resulting from the CAP3 program were aligned against the rat, mouse, and human Reference Sequence Project (RefSeq) databases[35,36] with BLASTn.[37] The e-value cutoff for the alignment was defined as 1e-50. The clusters aligning to the same RefSeq sequence were further merged into one cluster. The remaining clusters were then aligned against the rat, mouse, and human UniGene[38] and genomic databases with BLASTn at an e-value defined as 1e-20 and then further aligned with BLASTx alignment at an e-value cutoff of 1e-5.

Cluster Annotation

All clusters were annotated to RefSeq preferentially[35,36] and otherwise to UniGene. Rat, mouse, and human RefSeq were used as complementary annotation resources. If a cluster aligned to a RefSeq from a different species than rat, the RefSeq with lowest e-value alignment was selected as the annotation for the cluster. In cases in which the alignments between a cluster and a RefSeq from different species yielded the same e-value (e.g., e-value = 0.0), the priority order of annotation was rat>mouse>human.

dbEST Search

The sequences without a RefSeq or UniGene match were further aligned against rat, mouse, and human database for ESTs (dbEST)[39] with the same e-value cutoff (1e-20) applied.

Comparative Gene Expression Clustering

The RGC genes used for hierarchical clustering composed the subset of RGC clusters represented in the microarray data compiled by Su et al.[19] (http://expression.gnf.org/cgi-bin/index.cgi, Gene Expression Atlas, Genomics Institute of the Novartis Research Foundation, San Diego, CA) from 13 different neural regions. Replicate array data available for each region were first averaged. The *Cluster* and *TreeView* programs developed by Michael Eisen (http://rana.lbl.gov/EisenSoftware.htm; provided in the public domain by Eisen Lab, Lawrence Berkeley, national Lab, University of California at Berkeley) were then used for clustering and visualization, respectively. Both genes and neural regions were normalized by median centering and filtered for genes with expression in at least one neural region. Negative expression levels were set to zero. The parameters used for clustering were "absolute correlation" and "average linkage clustering."

Disease Loci

All sequence clusters were mapped to the human genome with an mRNA alignment program, SPIDEY.[40] The program was run with the interspecies alignment option on. The clusters falling into the disease loci were identified as disease candidate genes.

Immunohistochemistry

Eight-micrometer paraffin sections of rat retina were collected onto slides (Superfrost Plus; Fisher Scientific, Pittsburgh, PA) before immunolabeling by the streptavidin-biotin peroxidase method (Vector-SG detection kit; Vector Laboratories Inc., Burlingame, CA). Primary antibody was to RESP18 (a gift from Betty Eipper, University of Connecticut Health Center, Farmington, CT) or DDAH1 (a gift of Milan Vašák, Department of Biochemistry, Universität Zürich, Zürich, Switzerland). Negative controls included nonimmune serum of the same species as the primary antibody, or preimmune serum at the same protein concentration, or incubation buffer alone. Labeled sections were mounted in glycerol jelly and viewed by Nomarski optics (Axioskop; Carl Zeiss Meditec, Thornwood, NY).

Results

RGC Library Clones: Known and Novel

A nonnormalized, nonsubtracted cDNA library was constructed from purified postnatal day (P)21 rat RGCs. Generation of the library incorporated 16 rounds of PCR amplification to compensate for the limiting quantities of RNA available. The library contained 1.2×10^5 primary transcripts, with an average insert size of 1.8 kb. No further amplification of the library was performed. Five thousand clones were randomly selected for 5′ sequencing, generating 4791 usable EST sequences, with an average usable read length of approximately 500 bp.

Clustering of these ESTs to group together sequences representing the same transcript revealed 2360 unique gene clusters (complete listing available in Supplemental Table 1 at www.iovs.org/cgi/content/full/45/8/2503/DC1). Approximately 40% of the RGC library clones could be characterized as poorly characterized sequence, commonly termed ESTs. In a more detailed analysis, approximately 60% of the clusters (1408) represented known genes in the sense that they matched genes categorized in the NCBI Reference Sequence Project (RefSeq) sets for rat, mouse, and human genes. For the remaining 952 clusters a less stringent homology search was performed using UniGene for rat, mouse, and human. Approximately 60% of these clusters (n = 565) matched to UniGene clusters. Of the other 301 clusters, 92 matched to previously submitted EST sequences in dbEST. For each of the RGC clusters that matched only to otherwise unclassified dbEST ESTs, the tissue of origin of the matching dbEST ESTs was identified (Supplemental Table 1), to serve as a rough indication of the tissue types that express the gene.

The next step in the partitioning of RGC genes involved the 209 RGC clusters that had no match in the EST database by BLASTn. To characterize these remaining clusters further, and to select those most likely to represent rarely transcribed sequences, we aligned the clusters against the rat genome using BLAST. This alignment demonstrated that 82 of the clusters possessed two or more discontinuous areas of alignment on the genome, as would occur for exons of transcribed genes. In

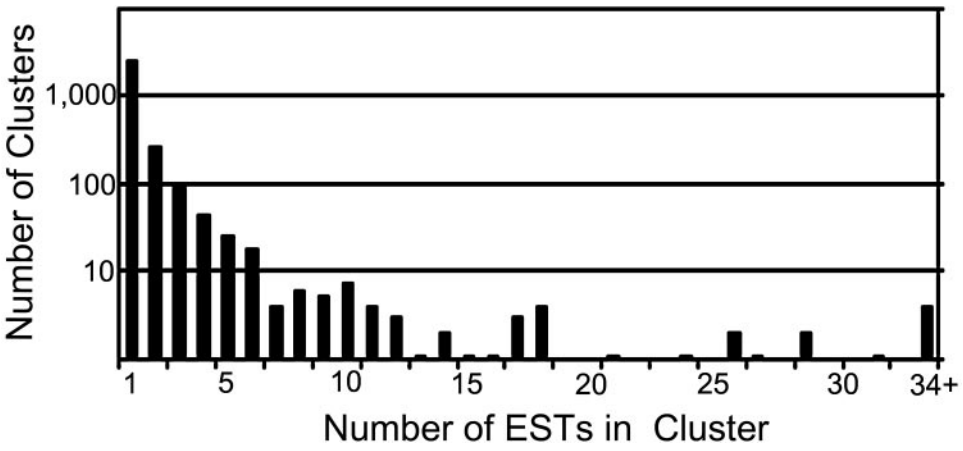

FIGURE 1. Cluster analysis for 4791 RGC ESTs. The histogram groups the EST clusters by size, from clusters made of only 1 EST sequence, to clusters containing 34 or more overlapping ESTs that collectively represent a single expressed sequence. Most (77%) of the ESTs had no significant sequence overlap with other RGC ESTs and so were in a cluster of size 1. As cluster size increased, the number of clusters at a given size decreased exponentially, reflecting the fact that fewer cellular genes are expressed at moderate and high levels.

agreement with this, most of these sequences, 73%, could be readily amplified by PCR. Of these 82 clusters with intron–exon structure, 74 showed no homology in the protein database or matched to predicted–theoretical protein records.

Library Representation of RGC Gene Expression

The distribution of RGC gene cluster size is shown in Figure 1. Most (77%) of the ESTs had no significant sequence overlap with other RGC ESTs,and so were in a cluster of size 1, as reflects the fact that most cellular mRNAs are expressed at low levels. As cluster size increased, the number of clusters at each increasing size was fewer, in an exponential-like decline, reflecting the fact that a smaller percentage of cellular genes are expressed at moderate levels, with fewer still expressed very highly. Though genes that are very highly expressed are few in number, they still account for a relatively large percentage of total mRNA produced by a cell, with the 10 largest RGC gene clusters containing approximately 500 of the 4791 total ESTs sequenced, or nearly 10% of the total (Table 1). We observed a strong inverse correlation between cluster size and the percentage of clusters that represented an unknown EST. For singleton clusters, as mentioned earlier, approximately 40% were ESTs. As cluster size increased, the percentage of ESTs decreased, from 32% for cluster size 2, to 16%, 8%, 6%, and 0% for cluster sizes between 3 and 6 or more, respectively.

Highly Expressed RGC Genes

Gene function assignments were made for the 100 most frequently sequenced RGC genes (Fig. 2). For this purpose, each gene was assigned to a single main category. Despite being highly represented, some genes have poorly understood functions. Nevertheless, functional assignments were possible for most genes in this group.

The protein modification enzyme ubiquitin was the single most frequently sequenced RGC gene, second only to the combination of mitochondria-encoded proteins. Of the 13 proteins encoded by the mitochondrial genome, 12 were sequenced from the RGC library (Table 2). The number of ESTs encountered for each of these genes varied greatly, from 18 for the largest cluster (ATP synthase F0 subunit 6) to NADH dehydrogenase subunit 3, which was not encountered at all. Mitochondrial mutations lead to selective RGC death in Leber's optic neuropathy, suggesting that mitochondrial gene expression levels may be particularly important in ganglion cell function. We therefore compared the cluster size found in the RGC library for each mitochondria-encoded gene to the cluster size in a non-normalized, nonsubtracted cDNA library (dbEST library ID.8847) from rat dorsal root ganglia, a cell type with similarities to RGCs that does not significantly degenerate in Leber's optic neuropathy. Although our sample size was small, there was a good overall correlation between cluster sizes for the mitochondria-encoded genes in the two cell types (R^2 =

TABLE 1. Large RGC Gene Clusters by Cluster Size

Mitochondrial proteins (226)	Tubulin beta 15 (21)
Polyubiquitin (151)	Heat shock cognate protein 70 (19)
Calretinin (74)	Selenoprotein W (18)
Peptidylprolyl isomerase A (62)	Malate dehydrogenase (18)
Alpha-tubulin (61)	Calmodulin 1 (17)
Aldolase C (56)	Transgelin 3 (17)
Calmodulin 2 (36)	Aldolase A (17)
H+ transporting ATPase, lysosomal 16 kDA (34)	Peroxiredoxin 2 (15)
Synaptic vesicle glycoprotein 2b (33)	Enolase 1 alpha (15)
Transcription elongation factor B 15 kDa (30)	Lactate dehydrogenase B (14)
Stathmin 1 (29)	Heat shock factor binding protein 1 (13)
SNAP25 interacting protein 30 (26)	Synuclein alpha (13)
Synuclein gamma (24)	Interferon alpha–inducible 27-like (13)
Microtubule-associated proteins 1A/1B light chain 3 (21)	Lactate dehydrogenase A (13)
	Regulated endocrine-specific protein 18 (12)
Thymus cell surface antigen, Thy1 (21)	Guanine nucleotide–binding protein gamma 3 (12)
Synaptic glycoprotein SC2 (21)	Myosin light polypeptide 6 (11)
Synaptosomal-associated protein Snap25 (21)	Triosephosphate isomerase 1 (11)
Heat shock protein 84 kDa 1 (21)	

The largest gene clusters from the RGC library, as defined by number of ESTs sequenced from the library in each cluster. Cluster size is indicated in parenthesis next to the gene name.

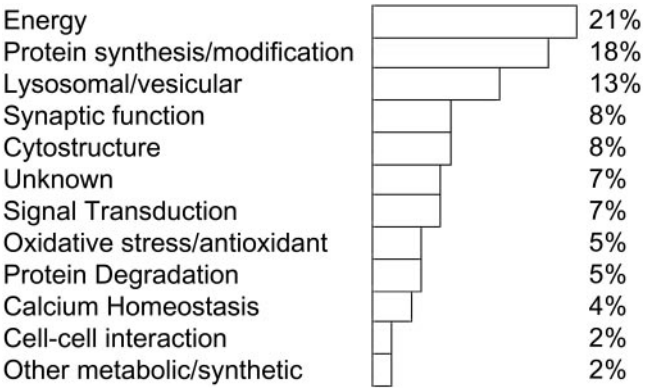

FIGURE 2. Gene ontogeny of the 100 most frequently sequenced RGC clones. Each gene was assigned to a single category corresponding to the main functional role of the gene, as determined by literature review.

0.4; Fig. 3), and thus no evidence of large differences in expression levels of mitochondria-encoded genes between RGC and DRG cells.

Also highly expressed in RGC cells were glycolytic and citric acid cycle enzymes, including malate dehydrogenase, lactate dehydrogenase, aldolase C, and aldolase A. These proteins are also highly represented in SAGE results from brain and retina,[7,8] and represent large clusters in UniGene, reflecting broad expression in many different tissues. Calcium-binding proteins were frequently encountered in the library, including calmodulin-1, -2, and -3; calretinin; calpactin 1; and calcyclin. Antioxidant genes were also prominent, including peroxiredoxin, glutathione *S*-transferase, and the poorly characterized selenoprotein W. After the five most represented functional categories (energy, protein synthesis/modification, lysosomal/vesicular, synaptic function, cytostructure), the next largest group was ESTs without known function.

Photoreceptor-specific genes are among the most frequently encountered ESTs in cDNA libraries made from whole retina, whereas in contrast in the RGC ESTs they were almost entirely excluded. For example, no ESTs were encountered for rhodopsin, transducin, or rod photoreceptor cGMP phosphodiesterase subunits. Similarly, no clones were encountered in the RGC library for Müller cell genes, such as cellular retinaldehyde-binding protein (CRALBP), vimentin, or glutamine synthase.

TABLE 2. Mitochondria-Encoded Genes

RGC Cluster Size	Protein Accession	Mitochondrial Proteins
18	NP_007230	ATP synthase F0 subunit 6
16	NP_007237	Cytochrome b
15	NP_007226	NADH dehydrogenase subunit 2
14	NP_007231	Cytochrome c oxidase subunit III
12	NP_007228	Cytochrome c oxidase subunit II
6	NP_007227	Cytochrome c oxidase subunit I
3	NP_007225	NADH dehydrogenase subunit 1
2	NP_007234	NADH dehydrogenase subunit 4
2	NP_007236	NADH dehydrogenase subunit 6
2	NP_007233	NADH dehydrogenase subunit 4L
1	NP_007229	ATP synthase F0 subunit 8
1	NP_007235	NADH dehydrogenase subunit 5

Mitochondria-encoded genes found in RGC library, in order of cluster size. Of the 13 proteins encoded by the mitochondrial genome, clones representing 12 were sequenced (no clone was encountered for NADH dehydrogenase subunit 3).

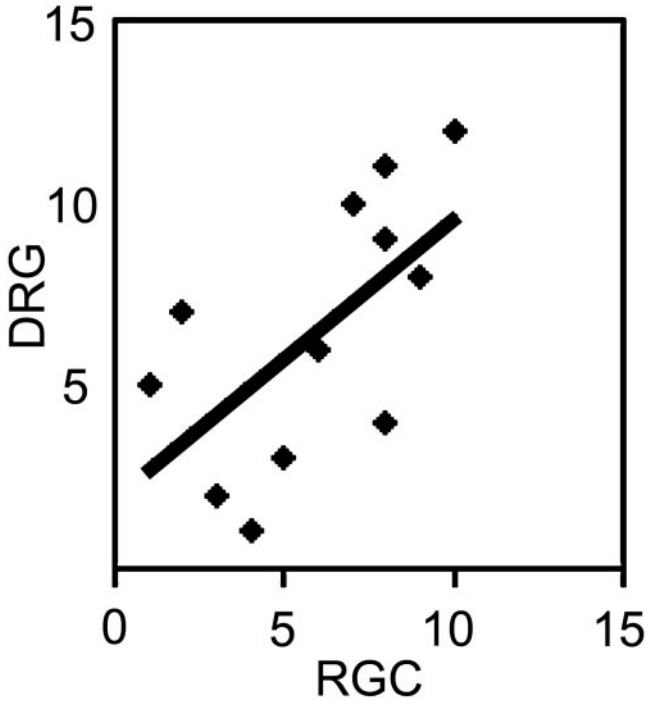

FIGURE 3. Scatterplot showing similar expression levels (as represented by cluster size) of mitochondria-encoded genes in the RGC library compared with a library derived from dorsal root ganglion (DRG) cells (dbEST Library ID.8847,[41]). The 13 mitochondria-encoded genes were assigned rank-order values (1–13) based on the number of ESTs/cluster in each library ($R^2 = 0.4$).

Neural- and Disease-Associated Gene Expression in RGCs

Surprisingly, a neuroendocrine-specific gene with poorly understood function, RESP18, was one of the most frequently encountered genes in the RGC library. We used immunohistochemistry to correlate RESP18 message found in the library with protein expression in the retina, and to localize its cellular expression pattern. RESP18 immunoreactivity was observed mainly in the RGC layer, with faint labeling of the inner plexiform layer and inner nuclear layer (Fig. 4). Staining was present mainly in cell bodies, in a perinuclear distribution consistent with its previously identified localization to the lumen of the endoplasmic reticulum.[42]

The functions of the remaining RGC clusters were then examined for genes that might be involved in pathways particularly important to RGC disease. One of the singleton genes, DDAH1, has been investigated for its involvement in nitric oxide metabolism[43–46] and neuronal injury. We found immunoreactivity for DDAH1 to be present in RGC and amacrine cell layers (Fig. 5). The sublaminae of the inner plexiform layer were particularly intensely immunoreactive, as was the retinal pigment epithelium.

Comparative Gene Expression Profiling of RGC Genes

Just as knowing which genes are expressed by RGCs should be informative of cell function, knowing the different neuronal types that express a gene should be informative of gene function. We therefore sought to determine where else in the nervous system genes expressed in RGCs were also expressed. Using hierarchical clustering to visualize expression patterns (Fig. 6), we compared our RGC data set to gene expression profiles generated using oligonucleotide microarrays from 13 separate neuronal regions[19] (http://expression.gnf.org/cgi-bin/

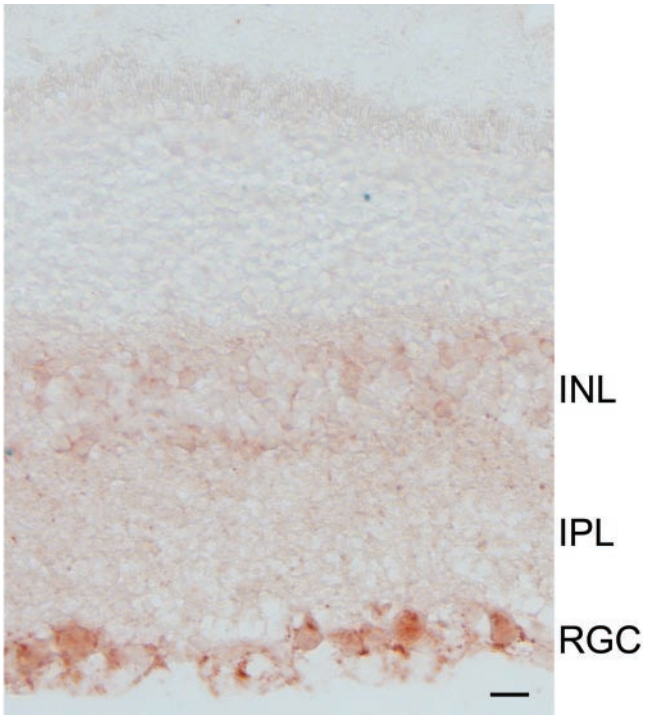

FIGURE 4. Expression of RESP18 in rat retina. RESP18 immunoreactivity was present mainly in large cell bodies in the ganglion cell layer, with faint immunoreactivity in the inner plexiform and inner nuclear layers and negligible labeling elsewhere. Immunoperoxidase staining with *brown* 3-amino-9-ethylcarbazole (AEC) reaction product. INL, inner nuclear layer; IPL, inner plexiform layer; RGC, retinal ganglion cell layer. Bar, 15 μm.

index.cgi). Of the 2360 RGC gene clusters, 959 were represented on these arrays, with 89% (851/959) showing positive signal in at least one neural area. A major resultant feature of the clustering was a subgroup of 24 genes relatively overexpressed in both dorsal root and trigeminal ganglia (Fig. 6, large oval). These sensory ganglia overexpressed genes, along with numerical expression level data are shown in Table 3. Hierarchical clustering was also performed across neural regions, as indicated by the tree structure. For the subset of genes expressed in retinal ganglion cells, the dorsal root and trigeminal ganglia were more closely related to each other than to the other neural regions.

To further explore the prominent RGC expression of RESP18, we focused on the smaller subset of RGC genes shown through clustering to be overexpressed in hypothalamus (Fig. 6 small oval, Table 4). One of these genes, necdin, has been reported to be overexpressed in hypothalamus,[47,48] whereas another, secretogranin 2, has known neuroendocrine functions. Necdin is thought to play a role in cell cycle arrest in terminally differentiated neurons, and secretogranin 2 is one of the chromogranin family of proteins, involved in secretory granulogenesis and the sorting and processing of secretory proteins.

Candidate Optic Neuropathy Genes Expressed by RGCs

To aid in candidate gene approaches to finding optic neuropathy-associated genes, we mapped the RGC genes to syntenic regions of the human genome associated with the optic neuropathy–associated loci GLC1B,[49] GLC1C,[50] GLC1D,[51] GLC1F,[52] OPA2,[53] OPA4,[54] WFS2,[55] SCABD,[56] and ARTS[57] (Table 5).

DISCUSSION

We have established an initial gene expression profile of purified rat RGCs through the approach of EST sequencing. This has allowed us to ascribe to RGCs the expression of a large number of known and novel genes. Several hundred novel sequences were identified from our sampling of only a minority of total genes expressed by RGCs, suggesting that we still have much to discover about RGC gene expression, especially about those genes expressed at low levels.

Although novel sequences from cDNA libraries are often described as ESTs, the term has certain limitations. For example, it does not distinguish rare novel sequences from more common sequences that are as yet unnamed. We therefore undertook a more detailed analysis of RGC gene clusters based on the full information available in NCBI databases. The RefSeq collections represent stable, curated databases of genes that have been documented at a higher level of certainty than those found in other experimental gene collections such as UniGene. The RGC genes that matched RefSeq entries were therefore considered known genes for this analysis. It is important to note, however, that most genes in RefSeq remain largely uncharacterized and that some characterized genes have not, at present, been included in RefSeq. The UniGene sets are based on automated partitioning of EST data into an experimental set of unique genes, based on sequence alignment combined with evidence of polyadenylation. Thus, in general, the RGC genes that matched to UniGene, but not to RefSeq, represented genes that are poorly characterized, possibly because of low expression levels. Those RGC sequences so rare as not to be found even in UniGene may represent transcripts of particular interest for future study.

The RGC clones were randomly selected and sequenced from a non-normalized, nonsubtracted cDNA library. This methodology can provide approximate information about the relative expression level of genes, but must be considered with caution in this instance because PCR was used in library construction to compensate for the limited quantity of RGC RNA.

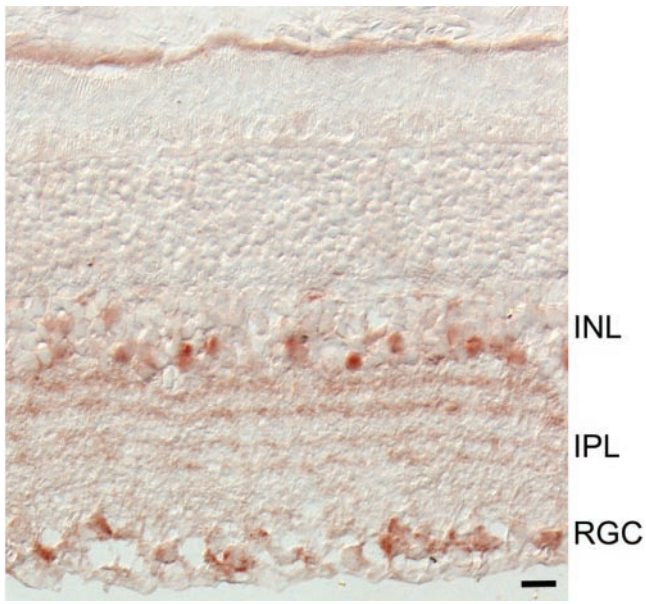

FIGURE 5. Expression of DDAH1 in rat retina. DDAH1 immunoreactivity was present in the ganglion cell layer, multiple sublaminae of the inner plexiform layer, and amacrine cell regions of the inner nuclear layer. Strong immunoreactivity was also present in the retinal pigment epithelium. Immunoperoxidase labeling with *brown* 3-amino-9-ethylcarbazole (AEC) reaction product. INL, inner nuclear layer; IPL, inner plexiform layer; RGC, retinal ganglion cell layer. Bar, 15 μm.

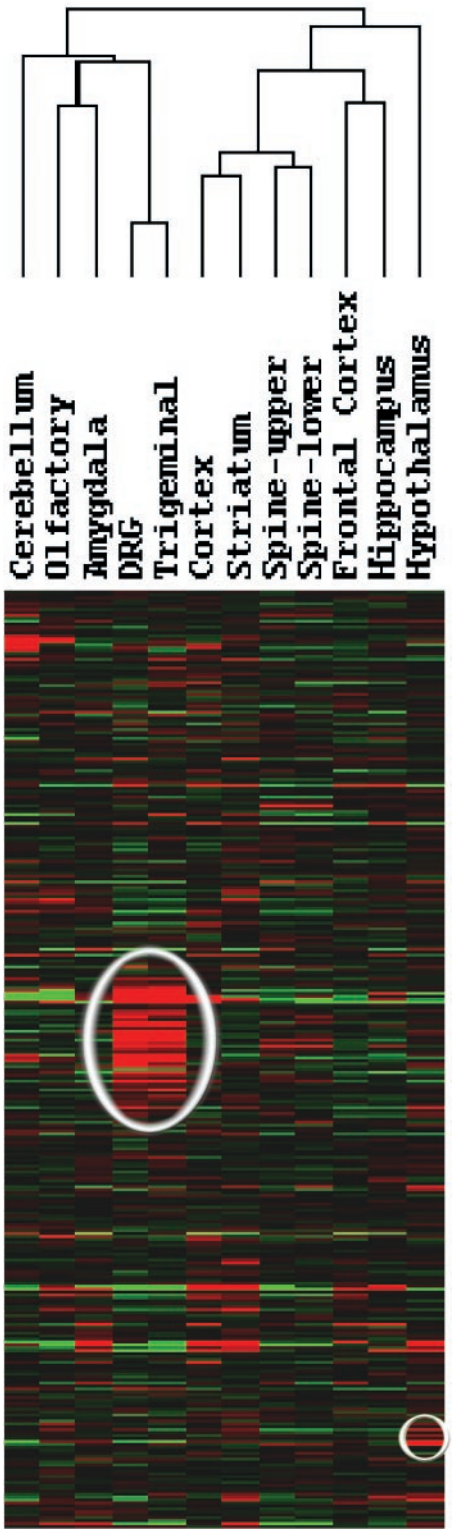

FIGURE 6. Comparative gene expression profiles of RGC genes. Comparison was made between the gene expression profile derived from RGCs through EST sequencing versus the gene expression profiles of 13 separate neuronal regions derived by Su et al.[18] using oligonucleotide microarrays. Hierarchical clustering is shown of the microarray output from the resultant 851 genes present in both ganglion cell and microarray data sets. Mean-centered normalization was applied across rows, so that *red* represents expression higher than average across the neural regions and *green* represents below average expression level. Overall brightness represents microarray signal intensity. Genes with similar expression patterns across neuronal areas are placed in proximity to each other. Genes relatively overexpressed in both dorsal root and trigeminal ganglia are indicated by the *large oval* and genes relatively overexpressed in hypothalamus are indicated by the *small oval*.

Several observations suggest that the rank ordering of genes we obtained may still be a useful representation of RGC gene expression levels: (1) In general, within any population of total mRNA, a small number of genes are highly abundant, with each of their individual mRNAs accounting for up to 1% of total cellular mRNA transcripts. For example, rhodopsin transcripts account for 1% or more of total retinal mRNA, and it is often the case that the 10 most highly expressed genes in a tissue account for approximately 10% of total mRNA. Such a distribution of highly expressed genes was encountered in this library, and included polyubiquitin and tubulin, among other genes expected to be highly expressed. (2) Along these same lines, nearly all genes in a tissue are of medium (0.1%–1%) or low abundance (0.1% or less of total mRNA).[58,59] Single EST sequences represented 77% of clusters in the RGC library, and the overall cluster size distribution was similar to that of a non-PCR amplified retinal cDNA library[11] as would be expected if the RGC library also contained a sampling of low-, medium-, and high-abundance mRNA species. (3) Mitochondria-encoded genes were expressed in the RGC library at ratios similar to levels in a non-PCR amplified library from dorsal root ganglion cells (Fig. 4). Lastly, (4) a strong correlation was present between RGC cluster size and the likelihood of the cluster's representing a known gene, as would be expected if highly expressed genes are more likely to be known, whereas low expression level genes are more likely to be unstudied ESTs.

Within the 35 genes most frequently sequenced from the RGC library (Table 1), a surprising number have poorly understood functions, and/or have not been studied in the retina. One of these for which there is some interesting information available is RESP18, which is expressed in endocrine and neural cells that secrete peptide hormones[60,61] and is suggested to be involved in intracellular signaling pathways.[62] In the brain, expression of RESP18 is limited to very specific regions, including the paraventricular and supraoptic nuclei of the hypothalamus, and the neurointermediate and anterior lobes of the pituitary. RESP18 is homologous to a region of the luminal domain of neuroendocrine-specific receptor-type protein tyrosine phosphatases and appears to be involved in intracellular signaling from the Golgi to the nucleus.[62] We speculate that further study of RESP18 may uncover a group of functionally interrelated genes that act within similar pathways in RGCs and the small subset of specialized neurons that preferentially express this gene.

Most mammalian genes remain poorly characterized, and similarly most of the genes we identified as singletons in the RGC library remain poorly characterized, both in general and in the retina. We selected DDAH1 for further study based on its involvement in nitric oxide metabolism, which has been particularly implicated in glaucomatous RGC death.[63–66] Also of interest, DDAH1 is increased in neurons with neurofibrillary tangles in Alzheimer disease[67]and in neuronal trauma.[68] DDAH1 hydrolyzes arginine residues that are asymmetrically methylated and endogenously generated. Such residues are competitive inhibitors of all three isoforms of nitric oxide synthase (NOS). Thus, inhibiting DDAH1 leads to decreased NO synthesis. This action may provide a therapeutic avenue for modulating NO levels in disease. The observation that DDAH1 is present both in the RGC and amacrine cell layers, as well as in multiple sublaminae of the inner plexiform layer, suggests a role for DDAH1 in ganglion and amacrine cell signaling.

TABLE 3. RGC Genes Overexpressed in Both Dorsal Root and Trigeminal Ganglia

	Cer	Olf	Amg	DRG	Trig	Cort	Stri	Sp-u	Sp-l	FroC	Hip	Hyp
Alpha-tubulin	5233	5528	4591	**10771**	**10154**	6491	4141	5638	5215	4154	5010	5782
Deleted in polyposis 1	759	1037	1762	**5658**	**4407**	1346	1311	1247	1205	1297	1222	1611
Calpain, small subunit 1	925	879	704	**3161**	**2162**	698	913	1087	1278	850	748	964
Serpinb6	31	21	110	**1986**	**1096**	80	56	187	266	99	154	115
Cathepsin L	282	357	183	**3294**	**2299**	182	181	347	467	212	276	507
S100a10	0	35	33	**3258**	**2100**	0	0	88	152	0	0	0
Synuclein, gamma	56	88	45	**6720**	**4595**	73	30	342	579	97	26	212
CD151 antigen	512	409	345	**1607**	**1436**	388	262	436	592	412	291	432
Chloride intracellular channel 1	26	0	0	**331**	**305**	0	0	0	23	0	0	0
Annexin A2	0	0	0	**7328**	**6987**	0	0	111	645	0	0	0
Annexin 5	508	808	378	**4929**	**4196**	717	875	1365	1362	697	458	907
Serping1	155	229	190	**919**	**816**	183	66	164	195	137	213	160
Proteasome 26s subunit	808	683	731	**1620**	**1435**	618	739	913	772	571	685	829
Riken 1110020C13	314	130	273	**825**	**612**	143	134	234	235	207	230	268
Stathmin-like 2	2791	1059	1845	**4942**	**5120**	2003	1441	2309	1954	1855	1453	2174
Aquaporin 1	225	324	311	**8859**	**9737**	179	52	1168	3885	145	897	203
CD59 antigen	21	39	64	**997**	**948**	0	99	237	337	81	125	130
CD151 antigen	512	409	345	**1607**	**1436**	388	262	436	592	412	291	432
Janus Kinase 1	128	30	83	**834**	**649**	209	168	391	308	16	163	142
Hmgcs1	352	480	642	**2537**	**1834**	721	724	1512	1047	619	470	879
HSC70	2510	2151	2642	**5251**	**4385**	2222	2612	3346	2663	2283	2047	3224
COP9 subunit 5	364	377	363	**762**	**734**	411	343	467	444	411	323	451
Squalene epoxidase	224	445	391	**1114**	**954**	438	297	590	549	349	373	541
FK506 binding protein 4	1340	845	522	**2053**	**1584**	506	523	586	673	565	393	578

Data are derived from hierarchical clustering of genes found in the RGC library that were also present in gene expression data derived by microarray analysis of 13 different neural regions. Data are non-normalized signal intensities from the microarrays (Affymetrix, Santa Clara, CA), except for assignment of zero to negative values. Cer, cerebellum; Olf, olfactory lobe, AMG, amygdala; DRG, dorsal root ganglia; Trig, trigeminal ganglia; Cort, cortex; Stri, striatum; Sp-u, upper spinal cord; Sp-l, lower spinal cord; FroC, frontal cortex; Hip, hippocampus; Hyp, hypothalamus. Shown in bold are RGC genes overexpressed in both dorsal root and trigeminal ganglia.

Several of the genes most frequently sequenced from the RGC library have been found to change expression in RGC injury. Synuclein gamma is increased in retinal glial cells in human glaucoma.[69] In an optic nerve crush model of ganglion cell death, stathmin showed reduced expression, whereas malate dehydrogenase and heat shock protein cognate 70 were both increased.[70]

Human genetic studies have identified several loci for inherited optic neuropathies. Candidate gene approaches to finding the specific gene causing these RGC diseases will be aided by knowledge of which genes in mapped loci are in fact expressed by RGCs (recognizing that a gene causing RGC death need not be expressed by RGCs). Of the RGC-expressed genes in these regions (Table 5), those known to be involved in neuronal degenerations or that are specifically expressed in neurons may be stronger candidates for RGC disease. Thus, the OPA4 region contained an "EST similar to ELAV (Embryonic lethal abnormal vision)-type RNA-binding protein 3" as annotated by NCBI. The ELAV family of genes is essential for *Drosophila* visual system development, and autoimmunity to these proteins can cause encephalomyelitis with sensory neuropathy.[71] Also within the OPA4 region was Ras-like without CAAX/Rin/Rit2, a small guanosine triphosphate (GTP)–binding protein that is expressed exclusively in neurons and in the retina is found only in ganglion cells and in the inner nuclear layer.[72,73] The GLC1D region similarly contained a neuron-restricted gene, potassium channel alpha subunit (Kv8.1). This gene has been analyzed in a positional candidate approach for adult familial myoclonic epilepsy, but without findings of pathogenic changes.[74]

One way to understand how the genome influences cell function is to compare the gene expression profiles among different cell types. This approach is amenable to high-throughput methods, such as EST sequencing, microarrays, and SAGE,

TABLE 4. Hypothalamus Overexpressed Genes in RGCs

	Cer	Olf	Am	DR	Trig	Cort	Stri	Sp-u	Sp-l	Fro	Hip	Hyp
Nascent polypeptide–associated complex alpha	981	1040	953	884	1104	818	1179	1118	1043	930	854	**1463**
Ribosomal protein L6	1977	2170	2437	2206	2874	2323	2399	2456	2425	2363	2267	**3230**
Melanoma antigen D1	594	1448	1812	1259	1753	1262	1451	1196	1198	1366	1681	**2721**
Centrin 2 (Cetn2)	0	34	118	79	95	9	26	34	58	24	76	**145**
Necdin (Ndn)	1853	901	2188	1749	769	1624	1697	1317	1389	1304	1628	**4602**
Secretogranin 2 (Scg2)	333	1609	865	980	776	746	1098	872	725	611	418	**2691**
Riken cDNA 6330403K07	6	1535	1496	522	321	1422	1450	1014	1043	1271	985	**4696**
Paternally expressed 3	682	918	885	810	631	705	1100	943	1012	820	598	**2074**
Regulated endocrine-specific protein 18	187	256	665	569	816	469	426	1062	938	535	390	**3109**
Ras-like without CAAX 2	284	221	206	286	215	120	234	652	419	169	180	**933**
Chromobox homolog 5	313	384	435	356	246	404	524	423	366	414	359	**617**

Data are derived from hierarchical clustering of genes in the RGC library that were also present in gene expression data derived by microarray analysis of 13 different neural regions. Data are signal intensities from the microarrays (Affymetrix). Regulated endocrine-specific protein 18, which was one of the largest gene clusters found in the RGC library, shows signal intensity in the hypothalamus almost three times higher than any other neural region examined. Shown in bold are RGC genes overexpressed in hypothalamus. For key to abbreviations, see Table 3.

TABLE 5. Candidate Optic Neuropathy Genes Expressed by RGCs

GLC1B	
NM_031100.1	Ribosomal protein L10 (Rpl10)
NM_025379.1	Cytochrome c oxidase subunit VIIb (Cox7b)
NM_175838.1	Eukaryotic translation elongation factor 1 alpha 1 (Eef1a1)
NM_016774.1	ATP synthase, H+ transporting mitochondrial F1 complex, beta subunit (Atp5b)
NM_021261.1	Thymosin, beta 10 (Tmsb10)
NM_017101.1	Peptidylprolyl isomerase A (cyclophilin A) (Ppia)
NM_031099.1	Ribosomal protein L5 (Rpl5)
GLC1C	
NM_024351.1	Heat shock protein 8 (Hspa8)
Rn.3357	ATP synthase, H+ transporting, mitochondrial F0 complex, subunit c, isoform 1
NM_007951.1	Enhancer of rudimentary homologue (*Drosophila*) (Erh),
Rn.1425	RAB7, member RAS oncogene family
NM_053330.1	Ribosomal protein L21 (Rpl21)
NM_012497.1	Aldolase C, fructose-biphosphate (Aldoc)
NM_012963.1	High mobility group box 1 (Hmgb1)
NM_030873.1	Profilin II (Pfn2)
Rn.82741	Actin, beta
NM_013067.1	Ribophorin I (Rpn1)
GLC1F	
CF978681	EST
Rn.1463	Peptidylprolyl isomerase A (cyclophilin A)
CF978691	EST
NM_031113.1	Ribosomal protein S27a (Rps27a)
NM_013216.1	Ras homologue enriched in brain (Rheb)
GLC1D	
NM_021697.1	Neuronal potassium channel alpha subunit (Kv8.1)
WFS2	
CF978606	EST
NM_007410.1	Alcohol dehydrogenase 5 (class III), chi polypeptide (Adh5)
NM_008015.1	Fibroblast growth factor inducible 14 (Fin14)
NM_175838.1	Eukaryotic translation elongation factor 1 alpha 1 (Eef1a1)
NM_145455.1	Similar to transcription factor BTF3 (RNA polymerase B transcription factor 3) (LOC218490)
SCABD	
NM_013226.1	Ribosomal protein L32 (Rpl32)
Rn.999	Laminin receptor 1 (67kD, ribosomal protein SA)
Rn.37758	Putative protein phosphatase 1 nuclear targeting subunit
NM_008210.1	H3 histone, family 3A (H3f3a)
NM_031100.1	Ribosomal protein L10 (Rpl10)
Rn.2458	Class 1 beta-tubulin, complete cds
Rn.82741	Actin, beta
Mm.66	Ribosomal protein S4, X-linked
NM_027148.1	RIKEN cDNA 2310032N20 gene (2310032N20Rik)
NM_022891.1	Ribosomal protein L23 (Rpl23)
NM_019678.1	Trk-fused gene (Tfg)
NM_173119.1	Heat shock factor binding protein 1 (Hsbp1)
NM_025592.2	Ribosomal protein L35 (Rpl35)
Rn.880	Cytochrome c oxidase subunit Vla (liver)
NM_029632.1	Protein phosphatase 1, regulatory (inhibitor) subunit 11 (Ppp1r11)
NM_173102.1	Tubulin, beta 5 (Tubb5)
NM_130823.1	ATPase, H+ transporting, lysosomal (vacuolar proton pump) 16 kDa (Atp6l)
NM_017101.1	Peptidylprolyl isomerase A (cyclophilin A) (Ppia)
NM_013663.2	Splicing factor, arginine/serine-rich 3 (SRp20) (Sfrs3)
NM_031099.1	Ribosomal protein L5 (Rpl5)
NM_013762.1	Ribosomal protein L3 (Rpl3)
NM_000984.2	Homo sapiens ribosomal protein L23a (RPL23A)
CF979103	EST
OPA4	
Mm.5163	Ras-like without CAAX/Rin
NM_013721.1	Ribosomal protein L7a (Rpl7a)
Rn.23878	ESTs, Weakly similar to elav-type RNA-binding protein 3
OPA2	
NM_031144.1	Actin, beta (Actb)
NM_029814.1	RIKEN cDNA 2210412K09 gene (2210412K09Rik)
NM_013226.1	Ribosomal protein L32 (Rpl32)
Rn.999	Laminin receptor 1 (67kD, ribosomal protein SA)
NM_012963.1	High mobility group box 1 (Hmgb1)
NM_031683.1	SMC-like 1 (yeast) (Smc1l1)
NM_008015.1	Fibroblast growth factor inducible 14 (Fin14)
NM_013721.1	Ribosomal protein L7a (Rpl7a)
NM_025449.1	Nicolin 1 (Nicn1)
Rn.2890	Ribosomal protein S15a
NM_027439.1	ATPase, H+ transporting, lysosomal interacting protein 1 (Atp6ip2)

(*continues*)

TABLE 5 (*continued*). Candidate Optic Neuropathy Genes Expressed by RGCs

NM_172372.1	DNA segment, Chr X, Immunex 38, expressed (DXlmx38e)
NM_000984.2	Homo sapiens ribosomal protein L23a (RPL23A)
ARTS	
NM_027870.1	ALEX3 protein (Alex3-pending)
NM_139254.1	Tubulin, beta 3 (Tubb3)
NM_008210.1	H3 histone, family 3A (H3f3a)
NM_022934.1	DnaJ-like protein (Hsj2)
NM_031119.1	Sjogren syndrome antigen B (Ssb)
NM_022298.1	Alpha-tubulin (Tuba1)
NM_012497.1	Aldolase C, fructose-biphosphate (Aldoc)
NM_021766.1	Progesterone receptor membrane component 1 (Pgrmc1)
NM_019979.1	Selenoprotein K (Selk-pending)
NM_145629.1	Expressed sequence AI115446 (AI115446)
Rn.1463	Peptidylprolyl isomerase A (cyclophilin A)
NM_026007.2	RIKEN cDNA 2610301D06 gene (2610301D06Rik)
NM_012570.1	Glutamate dehydrogenase 1 (Glud1)
NM_024351.1	Heat shock protein 8 (Hspa8)
Rn.2605	Thymosin beta-4
NM_007951.1	Enhancer of rudimentary homologue (*Drosophila*) (Erh)
NM_173119.1	Heat shock factor binding protein 1 (Hsbp1)
Rn.1463	Peptidylprolyl isomerase A (cyclophilin A)
NM_007451.2	Solute carrier family 25 (mitochondrial carrier; adenine nucleotide translocator), member 5 (Slc25a5)
CF978610	EST
NM_053297.1	Pyruvate kinase, muscle (Pkm2)
NM_023716.1	RIKEN cDNA 2410129E14 gene (2410129E14Rik)
NM_017101.1	Peptidylprolyl isomerase A (cyclophilin A) (Ppia)
NM_013762.1	Ribosomal protein L3 (Rpl3)
NM_001696.2	Homo sapiens ATPase, H+ transporting, lysosomal 31kDa, V1 subunit E isoform 1 (ATP6V1E1)

Genes expressed in a rat RGC library that are located within regions of mapped human optic neuropathies. Left column shows the NCBI database number corresponding to the gene name at right. Because several NCBI numbers can describe a single sequence, preference for inclusion in the table was given to RefSeq>Unigene>Genbank accession numbers. GLC1B, glaucoma 1, open angle, B; GLC1C, glaucoma 1, open angle C; GLC1F, glaucoma 1, open angle F; GLC1D, glaucoma 1, open angle D; WFS2, Wolfram syndrome gene 2; SCABD, spinocerebellar ataxia with blindness and deafness; OPA4, optic atrophy 4; OPA2, optic atrophy 2; ARTS, ataxia, fatal x-linked, with deafness and loss of vision.

and is particularly useful for gaining an initial insight into the roles of the large number of mammalian genes for which no detailed studies have been undertaken. In general, genes that are expressed at high levels in one neuronal type, but not in others, are likely contributors to phenotypic differences. In contrast, genes expressed at similar levels across neuronal subtypes might be expected to perform general cellular or neuronal functions and not to have a large role in establishing phenotypic differences. We examined the expression profile of the RGC genes in 13 different neural regions, as determined by the oligonucleotide microarray analysis of Su et al.[19] It is known that RGCs and other sensory ganglia such as the dorsal root and trigeminal ganglia share transcription factors such as the Brn-3 family.[75] As a consequence, it has been proposed that these neurons share similar genetic regulatory hierarchies.[75] Consequently, it might be expected that the cells would show downstream gene expression patterns with some significant similarities. This, in fact, appeared to be the case, with hierarchical clustering of gene expression revealing a pattern of RGC genes that were preferentially expressed in both the dorsal root and trigeminal ganglia. Several of these genes were among the largest RGC clusters, including tubulin, synuclein gamma, stathmin-like 2, and HSC70. Ion channels were also prominent in this group, including chloride intracellular channel 1, annexin 5, calpactin 1, and aquaporin 1.

There are many RGC subtypes, some of which have properties such as photoreception that set them apart from others.[76–78] This suggests that diversity will be found in gene expression patterns, even among RGCs, and highlights the need for increasingly stringent cell-type separations for future gene expression studies. The method of RGC purification used in the present study did not specifically bias against particular RGC subtypes, and the yield and survival of RGCs suggests that a fairly representative sample of RGCs was obtained. As a consequence, those subtypes present in small numbers, such as photoreceptive RGCs, would have made little contribution to the overall gene expression profile obtained. It is important to consider that gene expression patterns can vary greatly between seemingly similar samples, even controlling for such factors as genetic background, age, sex, and environment.[79] The RGC population examined in the current study was collected at a single time point in the midmorning, and the expression of some genes may be altered at different circadian time points, for example. Similarly, the specific conditions during RGC purification and overnight culture probably affected the expression levels of some genes. Thus, instead of a single, static gene expression profile defining a cell type, it appears that a range of profiles, when combined, better illustrates the more dynamic nature of transcriptional control of cellular phenotype.

Acknowledgments

The authors thank Danielle Valenta and Mary Ellen Pease for technical assistance.

References

1. Sommer A, Tielsch JM, Katz J, et al. Racial differences in the cause-specific prevalence of blindness in east Baltimore. *N Engl J Med*. 1991;325:1412–1417.
2. Quigley HA. Number of people with glaucoma worldwide. *Br J Ophthalmol*. 1996;80:389–393.
3. Swaroop A, Zack DJ. Transcriptome analysis of the retina. *Genome Biol.* 2002;3:REVIEWS1022.
4. Wistow G. A project for ocular bioinformatics: NEIBank. *Mol Vis*. 2002;8:161–163.
5. Sinha S, Sharma A, Agarwal N, Swaroop A, Yang-Feng TL. Expression profile and chromosomal location of cDNA clones, identified from an enriched adult retina library. *Invest Ophthalmol Vis Sci*. 2000;41:24–28.

6. Katsanis N, Worley KC, Gonzalez G, Ansley SJ, Lupski JR. A computational/functional genomics approach for the enrichment of the retinal transcriptome and the identification of positional candidate retinopathy genes. *Proc Natl Acad Sci USA*. 2002;99: 14326–14331.
7. Sharon D, Blackshaw S, Cepko CL, Dryja TP. Profile of the genes expressed in the human peripheral retina, macula, and retinal pigment epithelium determined through serial analysis of gene expression (SAGE). *Proc Natl Acad Sci USA*. 2002;99:315–320.
8. Blackshaw S, Fraioli RE, Furukawa T, Cepko CL. Comprehensive analysis of photoreceptor gene expression and the identification of candidate retinal disease genes. *Cell*. 2001;107:579–589.
9. Chowers I, Liu D, Farkas RH, et al. Gene expression variation in the adult human retina. *Hum Mol Genet*. 2003;12:2881–2893.
10. Chowers I, Gunatilaka TL, Farkas RH, et al. Identification of novel genes preferentially expressed in the retina using a custom human retina cDNA microarray. *Invest Ophthalmol Vis Sci*. 2003;44: 3732–3741.
11. Mu X, Zhao S, Pershad R, et al. Gene expression in the developing mouse retina by EST sequencing and microarray analysis. *Nucleic Acids Res*. 2001;29:4983–4993.
12. Livesey FJ, Furukawa T, Steffen MA, Church GM, Cepko CL. Microarray analysis of the transcriptional network controlled by the photoreceptor homeobox gene Crx. *Curr Biol*. 2000;10:301–310.
13. Farjo R, Yu J, Othman MI, et al. Mouse eye gene microarrays for investigating ocular development and disease. *Vision Res*. 2002; 42:463–470.
14. Jeon CJ, Strettoi E, Masland RH. The major cell populations of the mouse retina. *J Neurosci*. 1998;18:8936–8946.
15. Ahmad KM, Klug K, Herr S, Sterling P, Schein S. Cell density ratios in a foveal patch in macaque retina. *Vis Neurosci*. 2003;20:189–209.
16. Hernandez MR, Agapova OA, Yang P, Salvador-Silva M, Ricard CS, Aoi S. Differential gene expression in astrocytes from human normal and glaucomatous optic nerve head analyzed by cDNA microarray. *Glia*. 2002;38:45–64.
17. Wahlin KJ, Grice EA, Hackam AS, et al. A method for analysis of gene expression in isolated mouse photoreceptor and Müller cells. *Mol Vis.* 2004;10:366–375.
18. Miki R, Kadota K, Bono H, et al. Delineating developmental and metabolic pathways in vivo by expression profiling using the RIKEN set of 18,816 full-length enriched mouse cDNA arrays. *Proc Natl Acad Sci USA*. 2001;98:2199–2204.
19. Su AI, Cooke MP, Ching KA, et al. Large-scale analysis of the human and mouse transcriptomes. *Proc Natl Acad Sci USA*. 2002;99: 4465–4470.
20. Bonaventure P, Guo H, Tian B, et al. Nuclei and subnuclei gene expression profiling in mammalian brain. *Brain Res*. 2002;943: 38–47.
21. Zhao X, Lein ES, He A, Smith SC, Aston C, Gage FH. Transcriptional profiling reveals strict boundaries between hippocampal subregions. *J Comp Neurol*. 2001;441:187–196.
22. Che S, Ginsberg SD. Amplification of RNA transcripts using terminal continuation. *Lab Invest.* 2004;84:131–137.
23. Pavlidis P, Noble WS. Analysis of strain and regional variation in gene expression in mouse brain. *Genome Biol.* 2001;2: RESEARCH0042.
24. Zirlinger M, Kreiman G, Anderson DJ. Amygdala-enriched genes identified by microarray technology are restricted to specific amygdaloid subnuclei. *Proc Natl Acad Sci USA*. 2001;98:5270–5275.
25. Lee CK, Weindruch R, Prolla TA. Gene-expression profile of the ageing brain in mice. *Nat Genet*. 2000;25:294–297.
26. Cho Y, Gong TW, Stover T, Lomax MI, Altschuler RA. Gene expression profiles of the rat cochlea, cochlear nucleus, and inferior colliculus. *J Assoc Res Otolaryngol*. 2002;3:54–67.
27. Zirlinger M. Selection and validation of microarray candidate genes from subregions and subnuclei of the brain. *Methods*. 2003;31: 290–300.
28. Dent GW, O'Dell DM, Eberwine JH. Gene expression profiling in the amygdala: an approach to examine the molecular substrates of mammalian behavior. *Physiol Behav*. 2001;73:841–847.
29. Barrett T, Xie T, Piao Y, et al. A murine dopamine neuron-specific cDNA library and microarray: increased COX1 expression during methamphetamine neurotoxicity. *Neurobiol Dis*. 2001;8:822–833.
30. Goldberg JL, Espinosa JS, Xu Y, Davidson N, Kovacs GT, Barres BA. Retinal ganglion cells do not extend axons by default: promotion by neurotrophic signaling and electrical activity. *Neuron*. 2002; 33:689–702.
31. Meyer-Franke A, Kaplan MR, Pfrieger FW, Barres BA. Characterization of the signaling interactions that promote the survival and growth of developing retinal ganglion cells in culture. *Neuron*. 1995;15:805–819.
32. Barres BA, Silverstein BE, Corey DP, Chun LL. Immunological, morphological, and electrophysiological variation among retinal ganglion cells purified by panning. *Neuron*. 1988;1:791–803.
33. Goldberg JL, Klassen MP, Hua Y, Barres BA. Amacrine-signaled loss of intrinsic axon growth ability by retinal ganglion cells. *Science*. 2002;296:1860–1864.
34. Huang X, Madan A. CAP3: A DNA sequence assembly program. *Genome Res*. 1999;9:868–877.
35. Pruitt KD, Katz KS, Sicotte H, Maglott DR. Introducing RefSeq and LocusLink: curated human genome resources at the NCBI. *Trends Genet*. 2000;16:44–47.
36. Pruitt KD, Maglott DR. RefSeq and LocusLink: NCBI gene-centered resources. *Nucleic Acids Res*. 2001;29:137–140.
37. Altschul SF, Madden TL, Schaffer AA, et al. Gapped BLAST and PSI-BLAST: a new generation of protein database search programs. *Nucleic Acids Res*. 1997;25:3389–3402.
38. Schuler GD, Boguski MS, Stewart EA, et al. A gene map of the human genome. *Science*. 1996;274:540–546.
39. Boguski MS, Lowe TM, Tolstoshev CM. dbEST: database for "expressed sequence tags." *Nat Genet*. 1993;4:332–333.
40. Wheelan SJ, Church DM, Ostell JM. Spidey: a tool for mRNA-to-genomic alignments. *Genome Res*. 2001;11:1952–1957.
41. Xiao HS, Huang QH, Zhang FX, et al. Identification of gene expression profile of dorsal root ganglion in the rat peripheral axotomy model of neuropathic pain. *Proc Natl Acad Sci USA*. 2002;99: 8360–8365.
42. Schiller MR, Mains RE, Eipper BA. A neuroendocrine-specific protein localized to the endoplasmic reticulum by distal degradation. *J Biol Chem*. 1995;270:26129–26138.
43. Bogumil R, Knipp M, Fundel SM, Vasak M. Characterization of dimethylargininase from bovine brain: evidence for a zinc binding site. *Biochemistry*. 1998;37:4791–4798.
44. Knipp M, Charnock JM, Garner CD, Vasak M. Structural and functional characterization of the Zn(II) site in dimethylargininase-1 (DDAH-1) from bovine brain: Zn(II) release activates DDAH-1. *J Biol Chem*. 2001;276:40449–40456.
45. Kimoto M, Tsuji H, Ogawa T, Sasaoka K. Detection of NG,NG-dimethylarginine dimethylaminohydrolase in the nitric oxide-generating systems of rats using monoclonal antibody. *Arch Biochem Biophys*. 1993;300:657–662.
46. MacAllister RJ, Parry H, Kimoto M, et al. Regulation of nitric oxide synthesis by dimethylarginine dimethylaminohydrolase. *Br J Pharmacol*. 1996;119:1533–1540.
47. Niinobe M, Koyama K, Yoshikawa K. Cellular and subcellular localization of necdin in fetal and adult mouse brain. *Dev Neurosci*. 2000;22:310–319.
48. Aizawa T, Maruyama K, Kondo H, Yoshikawa K. Expression of necdin, an embryonal carcinoma-derived nuclear protein, in developing mouse brain. *Brain Res Dev Brain Res*. 1992;68:265–274.
49. Stoilova D, Child A, Trifan OC, Crick RP, Coakes RL, Sarfarazi M. Localization of a locus (GLC1B) for adult-onset primary open angle glaucoma to the 2cen-q13 region. *Genomics*. 1996;36:142–150.
50. Wirtz MK, Samples JR, Kramer PL, et al. Mapping a gene for adult-onset primary open-angle glaucoma to chromosome 3q. *Am J Hum Genet*. 1997;60:296–304.
51. Trifan OC, Traboulsi EI, Stoilova D, et al. A third locus (GLC1D) for adult-onset primary open-angle glaucoma maps to the 8q23 region. *Am J Ophthalmol*. 1998;126:17–28.
52. Wirtz MK, Samples JR, Rust K, et al. GLC1F, a new primary open-angle glaucoma locus, maps to 7q35–q36. *Arch Ophthalmol*. 1999;117:237–241.
53. Assink JJ, Tijmes NT, ten Brink JB, et al. A gene for X-linked optic atrophy is closely linked to the Xp11.4-Xp11.2 region of the X chromosome. *Am J Hum Genet*. 1997;61:934–939.

54. Kerrison JB, Arnould VJ, Ferraz Sallum JM, et al. Genetic heterogeneity of dominant optic atrophy, Kjer type: Identification of a second locus on chromosome 18q12.2-12.3. *Arch Ophthalmol*. 1999;117:805–810.
55. El-Shanti H, Lidral AC, Jarrah N, Druhan L, Ajlouni K. Homozygosity mapping identifies an additional locus for Wolfram syndrome on chromosome 4q. *Am J Hum Genet*. 2000;66:1229–1236.
56. Bomont P, Watanabe M, Gershoni-Barush R, et al. Homozygosity mapping of spinocerebellar ataxia with cerebellar atrophy and peripheral neuropathy to 9q33-34, and with hearing impairment and optic atrophy to 6p21-23. *Eur J Hum Genet*. 2000;8:986–990.
57. Kremer H, Hamel BC, van den Helm B, et al. Localization of the gene (or genes) for a syndrome with X-linked mental retardation, ataxia, weakness, hearing impairment, loss of vision and a fatal course in early childhood. *Hum Genet*. 1996;98:513–517.
58. Bishop JO, Smith GP. The determination of RNA homogeneity by molecular hybridization. *Cell*. 1974;3:341–346.
59. Getz MJ, Birnie GD, Young BD, MacPhail E, Paul J. A kinetic estimation of base sequence complexity of nuclear poly(A)-containing RNA in mouse Friend cells. *Cell*. 1975;4:121–129.
60. Bloomquist BT, Darlington DN, Mains RE, Eipper BA. RESP18, a novel endocrine secretory protein transcript, and four other transcripts are regulated in parallel with pro-opiomelanocortin in melanotropes. *J Biol Chem*. 1994;269:9113–9122.
61. Darlington DN, Schiller MR, Mains RE, Eipper BA. Expression of RESP18 in peptidergic and catecholaminergic neurons. *J Histochem Cytochem*. 1997;45:1265–1277.
62. Schiller MR, Mains RE, Eipper BA. A novel neuroendocrine intracellular signaling pathway. *Mol Endocrinol*. 1997;11:1846–1857.
63. Franco-Bourland RE, Guizar-Sahagun G, Garcia GA, et al. Retinal vulnerability to glutamate excitotoxicity in canine glaucoma: induction of neuronal nitric oxide synthase in retinal ganglion cells. *Proc West Pharmacol Soc*. 1998;41:201–204.
64. Morgan J, Caprioli J, Koseki Y. Nitric oxide mediates excitotoxic and anoxic damage in rat retinal ganglion cells cocultured with astroglia. *Arch Ophthalmol*. 1999;117:1524–1529.
65. Neufeld AH, Hernandez MR, Gonzalez M. Nitric oxide synthase in the human glaucomatous optic nerve head. *Arch Ophthalmol*. 1997;115:497–503.
66. Neufeld AH, Sawada A, Becker B. Inhibition of nitric-oxide synthase 2 by aminoguanidine provides neuroprotection of retinal ganglion cells in a rat model of chronic glaucoma. *Proc Natl Acad Sci USA*. 1999;96:9944–9948.
67. Smith MA, Vasak M, Knipp M, Castellani RJ, Perry G. Dimethylargininase, a nitric oxide regulatory protein, in Alzheimer disease. *Free Radic Biol Med*. 1998;25:898–902.
68. Nakagomi S, Kiryu-Seo S, Kimoto M, Emson PC, Kiyama H. Dimethylarginine dimethylaminohydrolase (DDAH) as a nerve-injury-associated molecule: mRNA localization in the rat brain and its coincident up-regulation with neuronal NO synthase (nNOS) in axotomized motoneurons. *Eur J Neurosci*. 1999;11:2160–2166.
69. Surgucheva I, McMahan B, Ahmed F, Tomarev S, Wax MB, Surguchov A. Synucleins in glaucoma: implication of gamma-synuclein in glaucomatous alterations in the optic nerve. *J Neurosci Res*. 2002;68:97–106.
70. Wang AG, Chen CH, Yang CW, et al. Change of gene expression profiles in the retina following optic nerve injury. *Brain Res Mol Brain Res*. 2002;101:82–92.
71. Szabo A, Dalmau J, Manley G, et al. HuD, a paraneoplastic encephalomyelitis antigen, contains RNA-binding domains and is homologous to Elav and Sex-lethal. *Cell*. 1991;67:325–333.
72. Lee CH, Della NG, Chew CE, Zack DJ. Rin, a neuron-specific and calmodulin-binding small G-protein, and Rit define a novel subfamily of ras proteins. *J Neurosci*. 1996;16:6784–6794.
73. Wes PD, Yu M, Montell C. RIC, a calmodulin-binding Ras-like GTPase. *EMBO J*. 1996;15:5839–5848.
74. Sano A, Mikami M, Nakamura M, Ueno S, Tanabe H, Kaneko S. Positional candidate approach for the gene responsible for benign adult familial myoclonic epilepsy. *Epilepsia*. 2002;43:26–31.
75. Xiang M, Zhou L, Macke JP, et al. The Brn-3 family of POU-domain factors: primary structure, binding specificity, and expression in subsets of retinal ganglion cells and somatosensory neurons. *J Neurosci*. 1995;15:4762–4785.
76. Gooley JJ, Lu J, Chou TC, Scammell TE, Saper CB. Melanopsin in cells of origin of the retinohypothalamic tract. *Nat Neurosci*. 2001;4:1165.
77. Hattar S, Liao HW, Takao M, Berson DM, Yau KW. Melanopsin-containing retinal ganglion cells: architecture, projections, and intrinsic photosensitivity. *Science*. 2002;295:1065–1070.
78. Provencio I, Rodriguez IR, Jiang G, Hayes WP, Moreira EF, Rollag MD. A novel human opsin in the inner retina. *J Neurosci*. 2000; 20:600–605.
79. Blackshaw S, Kuo WP, Park PJ, et al. MicroSAGE is highly representative and reproducible but reveals major differences in gene expression among samples obtained from similar tissues. *Genome Biol*. 2003;4:R17.